

# Fructose-Derived Levan Nanoparticles Protect Against Osteoarthritis by Directly Blocking CD44 Activation

Chanmi Cho, Jin Sil Lee, Hyeryeon Oh, Li-Jung Kang, Yiseul Hwang, Sunyoung Chae, In-Jeong Lee, Seok Jung Kim, Hyunmin Woo, Seong-il Eyun, Ho Chul Kang, Won Il Choi,\* and Siyoung Yang\*

Although the development of several inflammatory diseases can be initiated in response to CD44 receptor signaling dysregulation, anti-CD44 antibody therapy has been discontinued in clinical trials owing to its severe adverse effects. Moreover, biocompatible materials that block CD44 are unknown. Here, self-assembled levan nanoparticles (LevNPs) through simple nanoprecipitation without chemical conjugation of biocompatible levan are developed. LevNPs are prepared through a simple nanoprecipitation without chemical conjugation; this results in particles with a consistently dispersed hydrodynamic diameter of approximately 230 nm. The physicochemical properties of LevNP are well-maintained even after long-term storage in a physiological buffer, suggesting that LevNPs are stable and useful for various biomedical applications. A protein array and an *in silico* LevNP-CD44 interaction assay reveal that LevNPs specifically bind to CD44. Importantly, CD44 is highly expressed in the cartilage of patients with osteoarthritis (OA). LevNPs showed no cytotoxicity and reduced catabolic factor expression in an OA mimic *in vitro*. Furthermore, intra-articular injection of LevNPs exhibited long-term retention ability in the knee joint and protection against posttraumatic OA cartilage destruction in mice with medial meniscus destabilization-induced OA. These results show that LevNPs are biocompatible and exhibit potential as a nanotherapeutic for protecting against OA pathogenesis by directly blocking CD44.

## 1. Introduction

CD44 is a glycoprotein and transmembrane protein that performs several functions depending on ligand binding.<sup>[1]</sup> Moreover, CD44 has been implicated in several diseases, including osteoarthritis (OA), cancer, lung inflammation, and vascular diseases.<sup>[1]</sup> OA is a refractory degenerative disease characterized by the degeneration of joint cartilage and subchondral bones, a decrease in articular-joint lubrication, and CD44-induced inflammation.<sup>[2]</sup> As their prevalence has increased in aging and obese populations, the incidence of joint diseases has also increased worldwide, with an estimated 40% of the individuals over 70 years of age suffering from joint diseases.<sup>[3]</sup> Although CD44 expression is used as a marker of various inflammatory diseases and CD44 is considered a therapeutic target, CD44 inhibitors are limited to hyaluronic acid (HA).<sup>[4]</sup> Although HA is a useful biocompatible material that can be used to treat

C. Cho, L.-J. Kang, Y. Hwang, H. C. Kang, S. Yang  
Department of Biomedical Sciences  
Ajou University Graduate School of Medicine  
Suwon 16499, Republic of Korea  
E-mail: yangsy@ajou.ac.kr

C. Cho, L.-J. Kang, S. Yang  
Department of Pharmacology  
Ajou University School of Medicine  
Suwon 16499, Republic of Korea

C. Cho, L.-J. Kang, S. Yang  
Degenerative InterDiseases Research Center  
Ajou University School of Medicine  
Suwon 16499, Republic of Korea

C. Cho, L.-J. Kang, S. Yang  
CIRNO  
Sungkyunkwan University  
Suwon 16419, Republic of Korea


J. S. Lee, H. Oh, W. I. Choi  
Center for Bio-Healthcare Materials  
Bio-Convergence Materials R&D Division  
Korea Institute of Ceramic Engineering and Technology  
Chungbuk 28160, Republic of Korea  
E-mail: choi830509@kicet.re.kr

J. S. Lee, H. Oh  
School of Materials Science and Engineering  
Gwangju Institute of Science and Technology  
123 Cheomdan-gwagiro, Buk-gu, Gwangju 61005, Republic of Korea

Y. Hwang, H. C. Kang  
Department of Physiology  
Ajou University School of Medicine  
Suwon 16499, Republic of Korea

S. Chae  
Institute of Medical Science  
Ajou University School of Medicine  
Suwon 16499, Republic of Korea

I.-J. Lee  
Three-Dimensional Immune System Imaging Core Facility  
Ajou University  
Suwon 16499, Republic of Korea

 The ORCID identification number(s) for the author(s) of this article can be found under <https://doi.org/10.1002/smll.202202146>.

DOI: 10.1002/smll.202202146

OA,<sup>[5]</sup> it has a short half-life because of the action of hyaluronidase in the body,<sup>[6]</sup> thereby limiting its clinical application. Further, HA cannot be self-assembled without chemical conjugation of lipophilic moieties and its mass production is difficult owing to the complex steps required.<sup>[7,8]</sup> To overcome these limitations, polymer-based nanomedicines have been developed using new materials.<sup>[9–11]</sup>

Levan is a polysaccharide comprising a  $\beta$ -D-fructose polymer wherein the fructose rings are linked via  $\beta$ -glycosidic linkages.<sup>[12]</sup> The amphiphilic properties of levan enable micelles to be fabricated in aqueous solutions through self-assembly.<sup>[13]</sup> Furthermore, levan is biocompatible, biodegradable, renewable, and exhibits strong adhesion abilities. Levan has also been used in various applications because of its drug delivery efficacy and antioxidant, antiviral, and anti-inflammatory properties.<sup>[12,14,15]</sup> However, the preparation of levan nanoparticles (LevNPs) to improve their stability and efficacy via nanoprecipitation, and the anti-inflammatory effects of levan in OA have not been reported.

Here, we developed LevNPs by nanoprecipitation through the self-hydrophobic interaction of the fructose backbone. The physicochemical and morphological properties of the developed LevNPs were analyzed. The stability of the LevNPs was monitored and the therapeutic efficacy of these NPs and their mechanisms of action were determined using in vitro and in vivo OA models. Herein, we propose an efficient therapeutic strategy for OA by directly blocking CD44 with LevNPs (Figure 1A).

## 2. Results and Discussion

### 2.1. Physicochemical Properties of LevNPs

We prepared LevNPs by inducing the formation of hydrophobic interactions between the fructose of levan and  $\beta$ -glycosidic linkages (Figure S1, Supporting Information) in an aqueous solution. Dynamic light scattering analysis of the LevNPs revealed a hydrodynamic size of 230 nm with a narrow distribution, and transmission electron microscopy (TEM) images confirmed a mostly uniform spherical shape with a similar size as that observed using dynamic light scattering (Figure 1B,C). The zeta potential of the LevNPs was negative (−10 mV) under aqueous conditions because of the presence of the hydroxyl group on the shell (Figure 1C). In the Attenuated Total Reflection Fourier Transform Infrared (ATR-FTIR) analysis (Figure S2, Supporting Information), the LevNPs showed peaks corresponding to the glycosidic linkage (C–O–C; at 1128, 1061, and 1019  $\text{cm}^{-1}$ ) and fructose rings (at 928 and 814  $\text{cm}^{-1}$ ). Further, wide peaks at approximately 3400  $\text{cm}^{-1}$  from the O–H bond and 2937  $\text{cm}^{-1}$  from C–H bond were observed.<sup>[16]</sup> Notably, LevNPs were first fabricated by nanoprecipitation using levan, which comprises

a fructose structure. The stability of LevNPs was analyzed in an aqueous solution of deionized water (DIW) and physiological solution (phosphate-buffered saline; PBS; pH 7.4) after lyophilization.<sup>[17]</sup> As shown in Figure 1D, the LevNP powders were easily resuspended in the two solutions, with no significant difference in their diameter, and showed a low polydispersity index (PDI; less than 0.2). Further, the long-term stability of LevNPs which contain numerous hydrogen bonds—under physiological conditions was evaluated in PBS. Minimal changes in the physical properties of LevNPs were observed after four weeks (Figure 1E), suggesting that LevNPs are stable and can be utilized in biomedical applications aimed at treating OA.

### 2.2. Anti-Inflammatory Activity of LevNPs

Before examining the cytotoxicity of LevNPs against chondrocytes, we analyzed the amount of residual dimethyl sulfoxide (DMSO) in LevNPs as DMSO was a part of the preparation process. As shown in Figure S3A, Supporting Information, the amount of residual DMSO in LevNPs was very low, that is, 0.06%, indicating very low toxicity as reported previously.<sup>[18,19]</sup> We evaluated the cytotoxicity of LevNPs and DMSO (control) against fibroblasts as reported previously.<sup>[20–22]</sup> As shown in Figure S3B, Supporting Information, 0.1% DMSO showed no cytotoxicity with over 90% cell viability and LevNPs with 0.06% residual DMSO also did not exhibit toxicity toward cells.

Although levan has been reported to be a biocompatible fructose polymer,<sup>[12]</sup> its cytotoxicity against chondrocytes is unknown. Therefore, the cytotoxicity of LevNPs toward chondrocytes was assessed; LevNPs did not cause cytotoxicity in dose-dependent manner evaluated (Figure 1F). Thus, LevNPs may be used at high concentrations to effectively treat chronic inflammation. The anti-inflammatory efficacy of LevNPs was evaluated in IL-1 $\beta$ -treated chondrocytes (Figure 1G). LevNPs decreased cyclooxygenase2 (COX2) expression in a dose-dependent manner. Therefore, we developed LevNPs to treat inflammatory diseases, particularly OA.

### 2.3. Interaction Between LevNPs and CD44

To further characterize the mechanisms of action of LevNPs in chondrocytes, we utilized the HuProt<sup>TM</sup> 3.1 human proteome microarray (CDI Laboratories, Mayaguez, Puerto Rico), which contains more than 21 000 human proteins, to identify proteins that directly bind to the LevNPs. Cy5-labeled LevNPs (Cy5-LevNPs) exhibited fluorescence (Ex/Em = 646/662 nm) without influencing the maximum UV–vis absorption peak of LevNPs (Figure S4A, Supporting Information). A GST antibody was used to probe all proteins spotted on the ChIPs, followed by incubation with an Alexa Fluor goat-anti-rabbit 546 conjugated secondary antibody (Figure 2A,B). The signal-to-noise ratio (SNR) value for each spot was obtained as the foreground-to-background signals normalized to the GST signal intensity. Using this proteome microarray, we identified CD44 as a direct interacting partner of the LevNPs, which showed an SNR > 1.0, in 653 single transmembrane receptors (Figure 2C). The presence of direct interaction between LevNPs and CD44 was supported

S. J. Kim  
Department of Orthopaedic Surgery  
College of Medicine  
The Catholic University of Korea  
Seoul 06591, Republic of Korea  
H. Woo, S.-i. Eyun  
Department of Life Science  
Chung-Ang University  
Seoul 06974, Republic of Korea

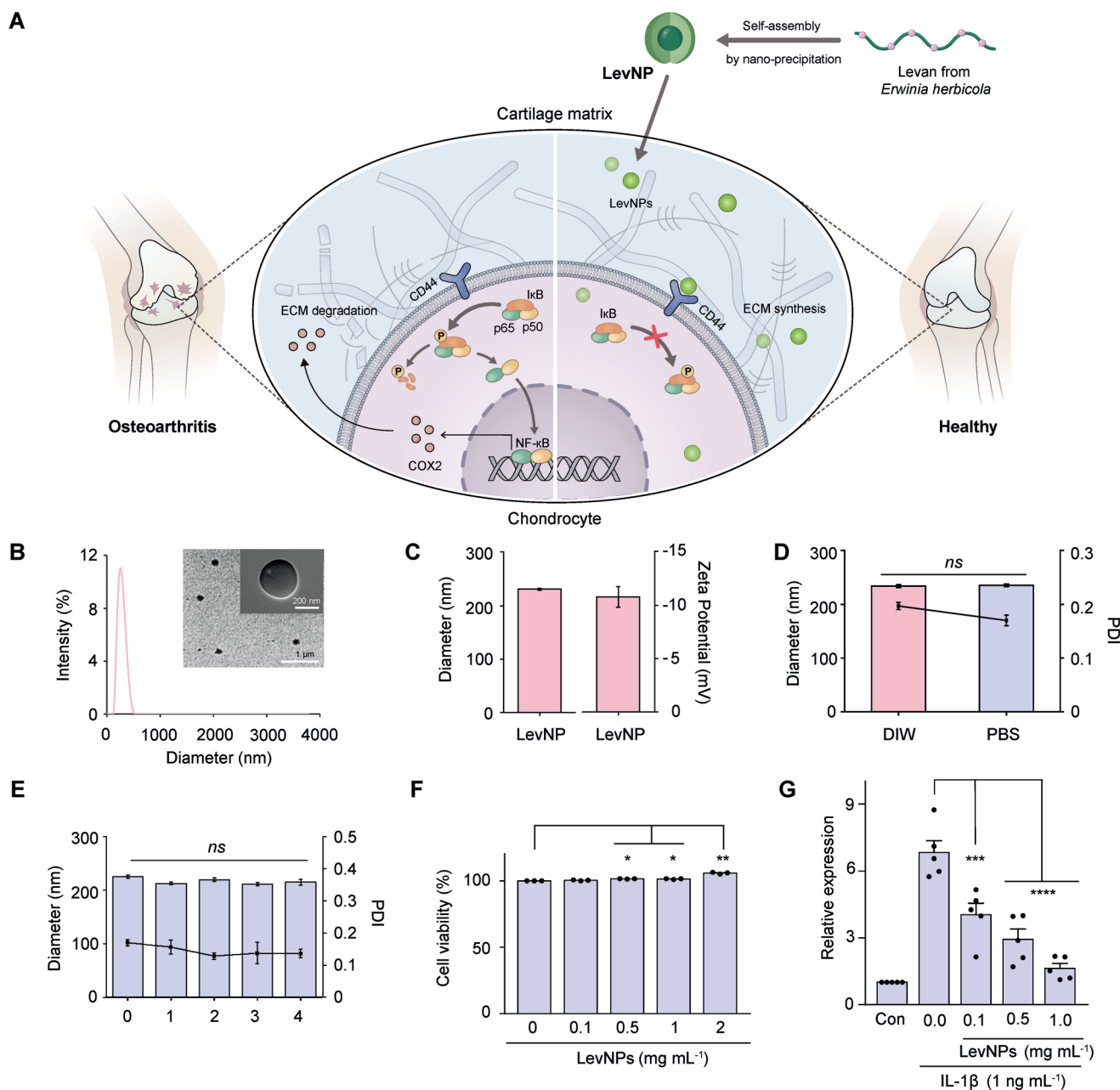


**Figure 1.** Physicochemical properties and stability analysis of LevNPs. A) A schematic representation of LevNP preparation and use in osteoarthritis treatment. B) Distribution peak and TEM images of LevNPs. Scale bars in TEM correspond to 200 nm and 1  $\mu$ m, respectively. C) Hydrodynamic diameter and zeta potential of LevNPs ( $n = 3$ ). D) Size and polydispersity index (PDI) of the re-suspension stability of LevNPs in aqueous solution (DIW) and physiological buffer (PBS) for storage ( $n = 3$ ). E) Long-term stability of LevNPs in physiological buffer (PBS) ( $n = 3$ ). F) In vitro cytotoxicity of LevNPs toward chondrocytes ( $n = 3$ ), and G) COX2 downregulation in response to different concentrations of LevNPs (qRT-PCR data) ( $n = 5$ ). Values are presented as the mean  $\pm$  SD, and were assessed using the D,E) Student's  $t$ -test and F,G) one-way ANOVA with Bonferroni's *post-hoc* test. \* $p < 0.05$ , \*\* $p < 0.01$ , and \*\*\* $p < 0.001$ .

by the results of in silico protein structural homology modeling (Figure 2D, left). CD44 is a transmembrane glycoprotein comprising an N-terminal domain, transmembrane domain, and cytoplasmic domain.<sup>[1]</sup> The N-terminal extracellular domain can bind various ligands, including hyaluronan, extracellular matrix glycoproteins, growth factors, and cytokines.<sup>[1]</sup> Our in silico analysis predicted that LevNPs bind to the N-terminal

residues E68, Y118, N121, and S123 of CD44 (Figure 2D, right), suggesting that LevNPs could block CD44-induced pathogenesis by the interactions of these amino acids of CD44.

As mentioned previously, HA is a well-known CD44 inhibitor that is used for treating OA. Kang et al. developed HA NPs through self-assembly and demonstrated that these NPs are promising therapeutic agents for OA.<sup>[23]</sup> However, despite the

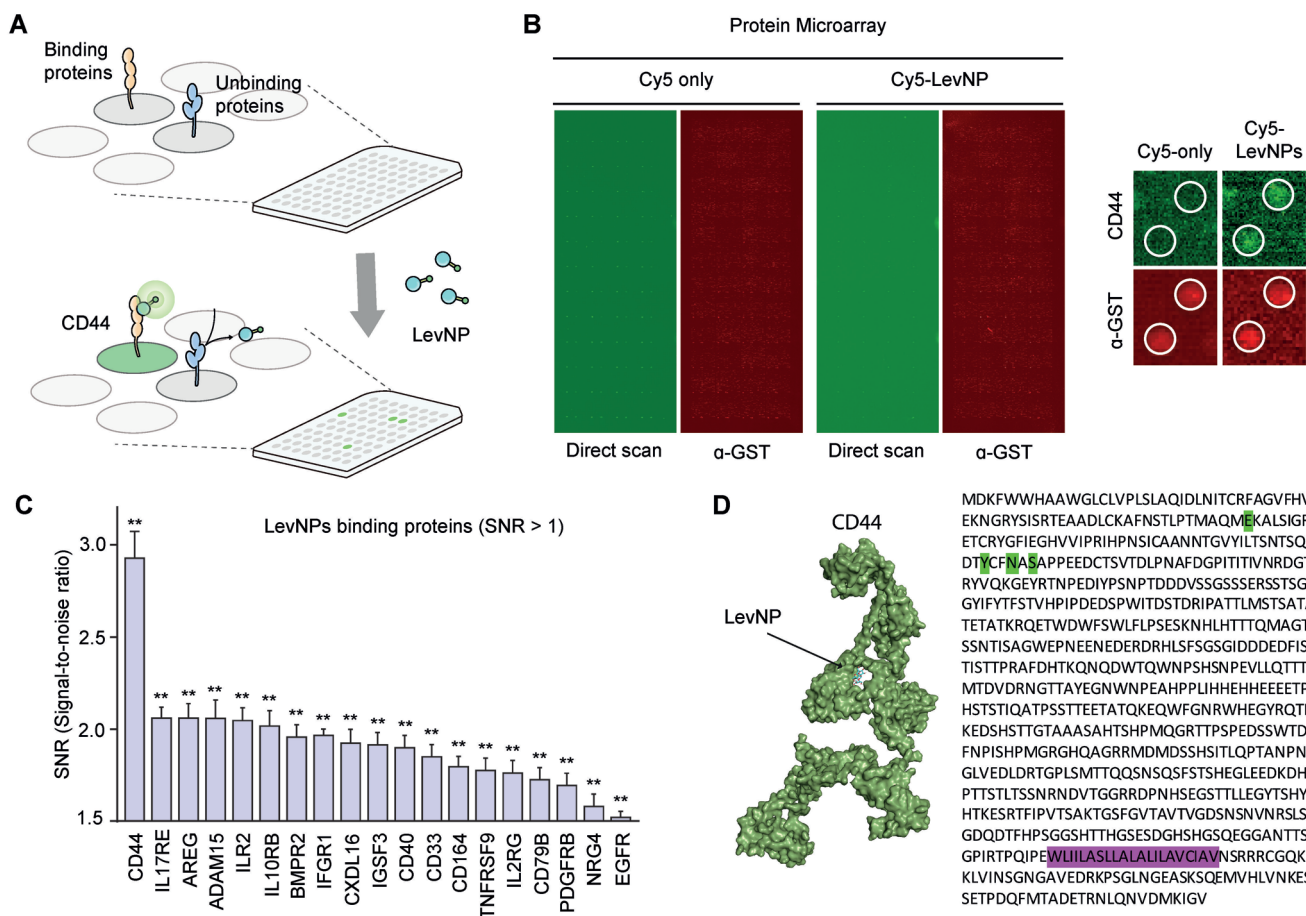


**Figure 2.** Identification of LevNP-binding proteins using a human protein microarray. A) Cy5 and Cy5-labeled LevNPs ( $5 \mu\text{g mL}^{-1}$ ) and LevNP-interacting proteins (green) were analyzed using HuProt<sup>TM</sup> 3.1 human protein ChIP. B) The signal-to-noise ratio (SNR) for each spot was determined as the ratio of the foreground-to-background signal. Further, the GST signal intensity (red) was used for SNR normalization (left). A high-power image of CD44 binding (white square boxes) is shown in the right panel. C) Nineteen proteins were identified as LevNP-interacting proteins and showed an SNR of greater than 1.0. The signal-to-noise ratio (SNR) was calculated using the following formula:  $\text{signal} = I_s$ ,  $\text{noise} = I_n$ ,  $\text{SNR} = 20 \log_{10} (I_s I_n^{-1})$ . Data are presented as the mean  $\pm$  SD (B, and C;  $n = 3$ ). D) Computational docking model for human CD44 (cyan) and LevNPs (olive) was predicted using the ClusPro 2.0 program (left). Pink: CD44 transmembrane (TM) domain. Green: LevNP-binding sites (right). Statistical comparisons were performed using a two-tailed Student's *t*-test, and  $p < 0.05$  was considered significant. \*\*  $p < 0.01$ .

general use of local HA injection for OA treatment, the use of these supplements is limited, as HA is unstable and rapidly degrades in the human body.<sup>[24]</sup> Although HA is non-covalently or covalently conjugated onto various nanocarriers to improve its stability, the system design is complex involving numerous synthesis steps, high costs, and challenges associated with the synthesis design for scale-up in an industrial setting. Moreover, acquiring the approval of the Food and Drug Administration may be difficult because of low biocompatibility.<sup>[25]</sup> Therefore, simply designed LevNPs were developed as novel CD44 inhibitors with good biodegradability and biocompatibility, low cost, and easy scale-up in industrial settings.

## 2.4. Blockade of CD44 Protects Catabolic Factor Expression During OA Pathogenesis

Although CD44 is expressed in the cartilage tissue,<sup>[2]</sup> its role in OA pathogenesis remains unclear. To characterize the role of

CD44 in OA pathogenesis, we performed in vitro and in vivo analyses. We analyzed the expression of CD44 in human OA cartilage and in the cartilage of mice with medial meniscus destabilization (DMM)-induced OA. As shown in **Figure 3**, CD44 expression in the damaged cartilage of human OA patients was higher than that in the undamaged control (Figure 3A) and OA mouse cartilage (Figure 3B). Next, we examined the role of CD44 in CD44 adenovirus (Ad-CD44)-infected mouse primary articular chondrocytes. COX2 is a critical factor in cartilage degeneration, a condition that is characterized by many up-regulated catabolic pathways and downregulated anabolic pathways.<sup>[23]</sup> Although COX2 is primarily involved in inflammation, further increased activation of matrix metalloproteinases eventually leads to the induction of Col2a1 degradation during OA development.<sup>[26]</sup> Transient expression of CD44 increased the COX2 levels (Figure 3C), indicating that CD44 induces the expression of catabolic factors in chondrocytes. Next, we investigated the role of CD44 in a mouse model of DMM-induced OA. WT and *CD44*<sup>-/-</sup> mice were subjected to DMM surgery (to



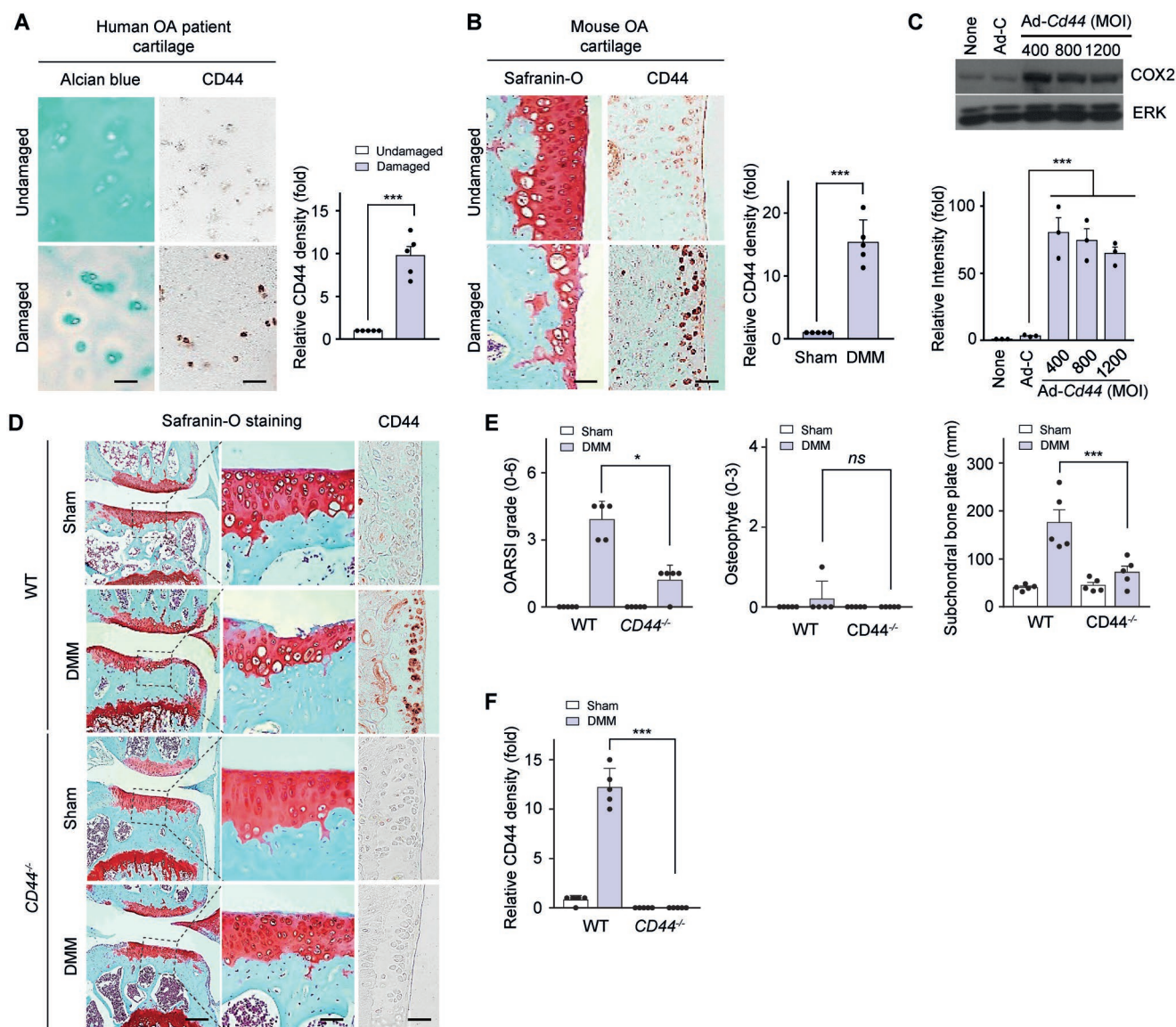


**Figure 3.** LevNPs block CD44-induced osteoarthritis (OA) pathogenesis. A) CD44 expression in OA cartilage samples from human patients (left) and relative densitometry (right). Scale bar, 100  $\mu$ m. B) Expression of CD44 in cartilage from mice with DMM-induced OA (left) and relative densitometry (right). Scale bar, 100  $\mu$ m. C) COX2 expression determined using western blotting (upper) and relative densitometry (lower) in Ad-CD44-transduced chondrocytes. D) Safranin-O staining and CD44 immunohistochemistry of OA cartilage from WT and CD44<sup>-/-</sup> mice. Scale bar, 100  $\mu$ m. E) Severity of cartilage destruction was evaluated based on the OARS I scores (left), osteophyte formation (middle), and subchondral bone thickness (right). F) Relative density of CD44 expression in cartilage from CD44<sup>-/-</sup> mice with DMM-induced OA. Values are presented as the mean  $\pm$  SD ( $n = 5$ ), and were assessed using A,B,F) two-tailed  $t$ -test, C,E) one-way ANOVA with Bonferroni's *post-hoc* test (subchondral bone plate thickness), and Kruskal–Wallis test followed by the Mann–Whitney U test (E; OARS I grading, and osteophyte formation). \* $p < 0.05$ , and \*\*\* $p < 0.001$ .

induce OA) or sham surgery (controls). Histological analyses revealed a lower degree of cartilage destruction in CD44<sup>-/-</sup> mice than that in WT mice (Figure 3D–F). Thus, CD44 is primarily involved in the pathogenesis of OA. Next, we investigated the role of LevNPs as CD44 inhibitors in OA pathogenesis. Using an ex vivo and in vivo OA mimic system, we demonstrated that LevNPs inhibited CD44 and COX2 expression, and may protect against inflammatory OA pathogenesis by blocking the expression of catabolic factors.

## 2.5. Penetration Efficacy and Function of LevNPs in Mouse Cartilage

Before characterizing the ex vivo and in vivo role of intra-articularly injected LevNPs in OA pathogenesis, we first examined the penetration efficacy and function of LevNPs in mouse cartilage. To test whether LevNPs can penetrate the cartilage matrix, we used ex vivo explant cartilage cultures from mouse joints. First, we demonstrated that Cy5.5 labeling did not affect

the characteristic UV-vis absorption peak of LevNPs in the near-infrared region (Figure S4B, Supporting Information). Explant cartilage was exposed to Cy5.5-LevNPs and free Cy5.5 for 24 h, after which the samples were observed using fluorescence microscopy. We confirmed that LevNPs substantially and actively penetrated the cartilage matrix, as evidenced by the high intensity and deep penetration of Cy5.5 in LevNPs-treated samples (Figure 4A). Moreover, to evaluate the duration of stable

retention of LevNPs in the synovium, Cy5.5-LevNPs and Cy5.5 (control) were injected into the mouse knee joints via intra-articular injection. Fluorescence microscopy revealed that the signals corresponding to LevNPs persisted for 48 h, whereas those corresponding to Cy5.5 disappeared readily (Figure 4B). The joints were collected to evaluate the stability and diffusion of LevNPs into the cartilage matrix. Remarkably higher intensity of Cy5.5 was observed in the Cy5.5-LevNPs-injected joints (compared to

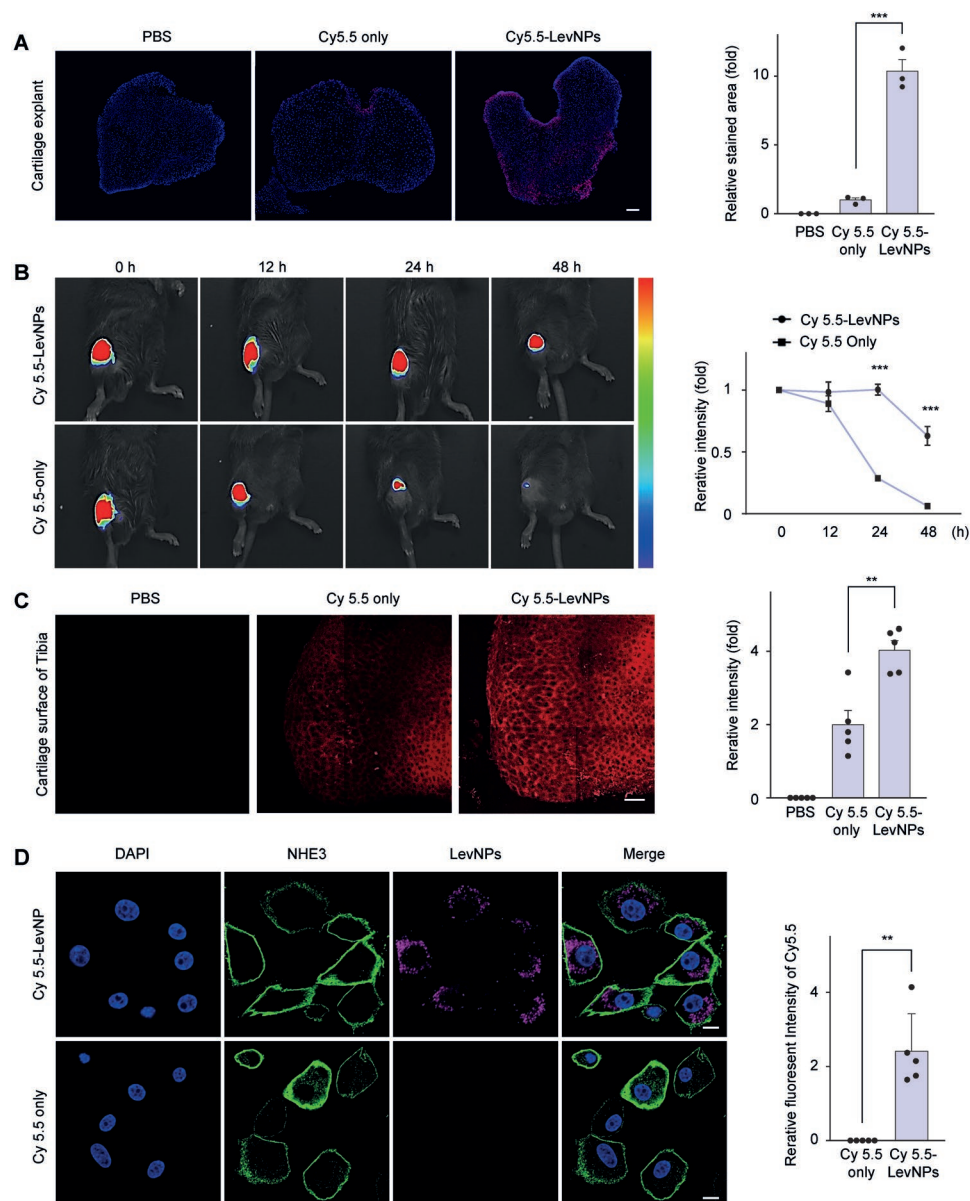


**Figure 4.** Long-term retention and active absorption of LevNPs in cartilage matrix. A) Fluorescence microscopy image of the mouse articular cartilage explant after exposure to free Cy5.5 and Cy5.5-labeled LevNPs for 24 h (left). Quantification of the fluorescence penetration depth (right). Scale bar, 100  $\mu$ m. B) Time-dependent image of Cy5.5-labeled LevNPs and free Cy5.5 intra-articular injected into the knee joint of C57BL/6 mice (left). Scale bar, 50  $\mu$ m. LevNPs were quantified in the knee joints based on relative fluorescence intensity (right). C) Fluorescence microscopy image of the mouse articular cartilage 6 h after the intra-articular injection of Cy5.5-labeled LevNPs (red). Scale bar, 20  $\mu$ m. Quantification of the fluorescence intensity of Cy5.5 (right;  $n = 5$ ). D) Immunofluorescence microscopy images of DAPI, NHE3 (membrane marker), and Cy5.5-labeled LevNP (left). Quantification of the fluorescence intensity of Cy5.5 (right;  $n = 5$ ). Values are presented as the mean  $\pm$  SD, and were assessed using the A,C,D) two-tailed  $t$ -test and B) one-way ANOVA with Bonferroni's *post-hoc* test. \*\*  $p < 0.01$ , and \*\*\*  $p < 0.001$ .

control), indicating high absorbance of the LevNPs in the cartilage matrix (Figure 4C).

The cytoplasmic domain of CD44 is known to be an important mediator of cellular internalization.<sup>[27]</sup> Gou et al. investigated a chondroitin sulfate-functionalized silk fibroin-based nanoscale drug delivery system and reported that the system alleviated ulcerative colitis by interacting with the overexpressed CD44 on the macrophage surface. Importantly, chondroitin sulfate enhanced the cellular uptake of curcumin by macrophages through CD44-mediated endocytosis.<sup>[28]</sup> Thus, this system can enhance the bioavailability and pharmacokinetics of curcumin both in vivo and in vitro.<sup>[28]</sup> We next checked whether chondrocytes could internalize the LevNPs. As shown in Figure 4D, we identified the internalization of LevNPs in chondrocytes. This suggested a potential mechanism for the modulation of CD44-mediated LevNP uptake.

## 2.6. Protection Against OA Pathogenesis via Intra-Articular Injection of LevNPs in Posttraumatic OA

We next evaluated whether LevNPs can be used as a therapeutic agent for OA with ex vivo conditions. In OA-mimicking ex vivo conditions, Alcian blue staining of IL-1 $\beta$ -treated explant cartilage revealed that the integrity of the ECM degradation was inhibited by LevNPs treatment (Figure 5A). We next checked whether LevNPs could recover ECM synthesis in IL-1 $\beta$ -treated explant cartilage. As shown in Figure 5B, decreased integrity of the cartilage ECM by IL-1 $\beta$  treatment was recovered upon LevNPs treatment, suggesting that LevNPs directly penetrate the cartilage tissues and promote ECM synthesis as well as blockade of ECM degradation. Next, we checked the function of LevNPs in an OA mouse model. The DMM mouse model mimics spontaneous human OA characterized by generating unstable meniscus support between the cartilage of the femur and tibia, thereby inducing spontaneous contact between these structures.<sup>[29]</sup> During OA pathogenesis, inflammation onset and cartilage destruction were observed 4–6 weeks after DMM surgery.<sup>[30]</sup> Four weeks after surgery, these mice were intra-articular injected with 50 mg kg<sup>-1</sup> LevNPs or PBS per knee (Figure 5C). Safranin-O staining revealed significantly reduced proteoglycan loss and cartilage erosion. Histological examination of the cartilage layer revealed typical inflammatory conditions associated with OA, which were alleviated in the LevNPs-injected group. Sections of the knee joint were scored blindly using the criteria used for grading inflammatory OA, for example, OARS1, osteophyte formation, and subchondral bone plate thickness (Figure 5D). The CD44 is the downstream target gene of NF- $\kappa$ B and cytoplasmic retention of NF- $\kappa$ B by I $\kappa$ B is the major mechanism that controls its activity.<sup>[2,31]</sup> We next check whether LevNPs block I $\kappa$ B degradation by  $\kappa$ B phosphorylation in the LevNPs-injected groups. The immunohistochemistry and immunofluorescence analysis revealed that the NF- $\kappa$ B pathway-mediated expression of COX2 in the articular cartilage of mice with DMM-induced OA was decreased following the intra-articular injection of LevNPs (Figure 5E, and Figure S5, Supporting Information), confirming that the LevNPs alleviate cartilage inflammation and degradation during OA progression.

## 3. Conclusion

We successfully prepared LevNPs through simple nanoprecipitation without chemical conjugation. These LevNPs were consistently dispersed and stable without any drastic changes in their hydrodynamic diameter or PDI in physiological buffer, PBS. Protein array and in silico protein binding analyses demonstrated that LevNPs bind to CD44, resulting in the blockade of OA pathogenesis through the inhibition of cartilage destruction and inflammation. Further, CD44 was highly expressed in the OA cartilage of humans and mice, and the LevNPs-mediated inhibition of CD44 expression resulted in the downregulated expression of catabolic factors in mouse articular chondrocytes. Moreover, LevNPs administered via intra-articular injection easily penetrated the cartilage tissues, were highly stable, and reduced IL-1 $\beta$ -induced degradation of the ECM under ex vivo explant cartilage culture conditions. Importantly, LevNPs protected against DMM-induced cartilage destruction by reducing the expression of CD44 and COX2. Thus, LevNPs may suppress OA pathogenesis in humans; however, further studies are needed to evaluate this hypothesis. LevNPs exhibit potential as safe and reliable agents for treating OA and CD44-mediated inflammatory human diseases. LevNPs loaded with specific drugs may further improve the therapeutic outcomes or exert multiple simultaneous effects, depending on the type of drug used.

## 4. Experimental Section

**Reagents:** Levan (molecular weight,  $\approx$ 1 MDa) from *Erwinia herbicola* and DMSO were purchased from Sigma-Aldrich (St. Louis, MO, USA). DIW and PBS (1x, pH 7.4) were purchased from Hyclone (Logan, UT, USA). Cy5 mono NHS ester and Cy5.5 mono NHS ester were obtained from Cytiva (Marlborough, MA, USA). For in vitro analysis, the mouse articular chondrocytes were cultured in Dulbecco's modified Eagle's medium (DMEM; Gibco, Grand Island, NY, USA) supplemented with 10% fetal bovine serum (FBS; Gibco) and penicillin-streptomycin (10 000 U mL<sup>-1</sup>; Thermo Fisher Scientific, Waltham, MA, USA). All reagents were used directly without further purification.

**Human OA Cartilage and Animals:** Human cartilage samples were obtained from individuals aged 45–65 years who underwent total knee arthroplasty after providing written informed consent (Table S1, Supporting Information). The study was approved by the Institutional Review Board of the Catholic University of Korea (UC14CNS10150). The undamaged portion of cartilage from human OA patients was defined as healthy cartilage. All animal experiments were approved by the Institutional Animal Care and Use Committee (IACUC-2019-0019) of Ajou University. Mice (male C57BL/6 and ICR) weighing 18–20 g were purchased from DBL (Chungcheongbuk-do, South Korea). The mice were housed in 200 (W)  $\times$  260 (D)  $\times$  130 mm (H) cages (maximum of four mice per cage) in an environmentally controlled room at 25  $^{\circ}$ C with humidity of approximately 50% and under a 12-hour light-dark cycle. Animals were provided ad libitum access to chow and water.

**Cell Culture:** In vitro analysis, NIH/3T3 (mouse embryonic fibroblast) cells acquired from ATCC (American Type Culture Collection; Manassas, VA, USA) were cultivated in DMEM (Dulbecco's modified Eagle's medium; Gibco, Grand Island, NY, USA) contained 10% fetal bovine serum (FBS) obtained Gibco and penicillin-streptomycin (10 000 U mL<sup>-1</sup>) obtained Thermo Fisher Scientific (Waltham, MA, USA). Mouse articular chondrocytes were obtained from the cartilage of C57BL/6 mice (5 days after birth). Mice were euthanized before dissection, and the femoral condyles and tibial plateaus of the mice were digested with 0.2% (w v<sup>-1</sup>)



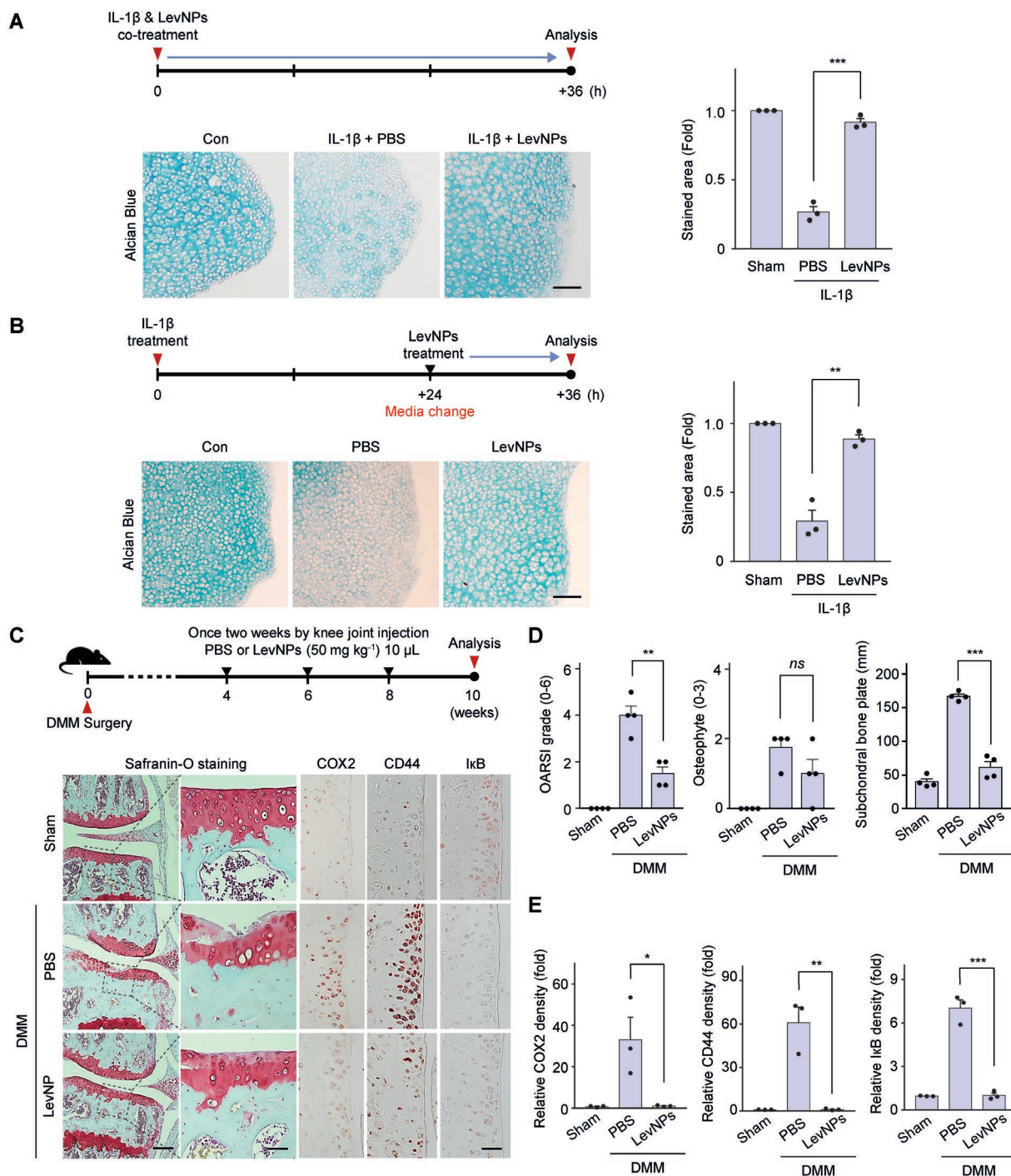


**Figure 5.** LevNPs alleviate osteoarthritis (OA) pathogenesis by blocking CD44-induced expression of COX2 via NF- $\kappa$ B regulation. A) Image depicting Alcian blue staining of ex vivo-cultured cartilage after exposure to IL-1 $\beta$  with LevNPs for 36 h (left). Quantification of the stained area (right) ( $n = 3$ ). B) Image depicting Alcian blue staining of LevNPs treated ex vivo-cultured cartilage for 12 h after IL-1 $\beta$  expose for 24 h (left). Quantification of the stained area (right) ( $n = 3$ ). C) Schematic depiction of intra-articular LevNPs injections 4 weeks after DMM surgery. Representative images of the histopathological changes in the cartilage 10 weeks after destabilization of the medial meniscus (DMM) surgery with intra-articular injection of PBS, and LevNPs injections, respectively ( $n = 5$ ). Changes in the expression of COX2, I $\kappa$ B, and CD44 with intra-articular injection of LevNPs evaluated using immunohistochemistry ( $n = 4$ ). Scale bar, 50  $\mu$ m. D) Cartilage degradation was quantified based on OARSI scores (left), osteophyte formation (middle), and subchondral bone thickness (right). E) Quantification of CD44, I $\kappa$ B, and COX2 expression in the cartilage ( $n = 5$ ). Values are presented as the mean  $\pm$  SD ( $n = 5$ ), and were assessed using A,B,E) two-tailed  $t$ -test, D) one-way ANOVA with Bonferroni's *post-hoc* test (subchondral bone thickness), Kruskal–Wallis test followed by the Mann–Whitney U test (D; OARSI grading, and osteophyte formation). \* $p < 0.05$ , \*\* $p < 0.01$ , \*\*\* $p < 0.001$ , \*\*\*\* $p < 0.0001$ .



collagenase type II and 0.1% (w v<sup>-1</sup>) trypsin (prepared in DMEM) for 3 h. The digested cartilage was isolated from its bonds and additionally digested with 0.1% (w v<sup>-1</sup>) collagenase type II for 2 h. The cells were filtered and seeded ( $2.8 \times 10^5$  cells mL<sup>-1</sup>) in 35 mm culture dishes followed by culture in DMEM supplemented with 10% FBS and 1% penicillin-streptomycin. The cells cultured for two days were treated as indicated in each experiment. For in vitro OA analysis, mouse articular chondrocytes were co-treated with LevNPs (0.1, 0.5, and 1 mg mL<sup>-1</sup>) and either IL-1 $\beta$  (1 ng mL<sup>-1</sup>) for 24 h.

**Preparation and Characterization of LevNPs:** LevNPs were prepared based on the hydrophobic interactions within the fructose backbone using simple nanoprecipitation. First, levan (10 mg) was dissolved in 1 mL DMSO, and allowed to react under rotary shaking for 2 h. The reacted liquid was added dropwise into 5 mL DIW with gentle stirring. After 1 h (to remove the DMSO), the solution containing the LevNPs was lyophilized for 3 days in a freeze dryer (LP20; Ilshin BioBase Co. Ltd., Gyeonggi-do, Korea). Furthermore, after resuspending the dried LevNPs in DIW (2 mg mL<sup>-1</sup>), the solution was purified, followed by centrifugation at 2000 rpm using Amicon Ultra-15 centrifugal filters (molecular weight cutoff = 100 kDa; Merck Millipore, Billerica, MA, USA) at 25 °C. To analyze the residual amount of the organic solvent in the LevNPs preparation, HPLC was performed. An HPLC system equipped with a C18 column (5  $\mu$ m; SunFire® C18 column, Waters Corp) was used with 70% acetonitrile as the mobile phase. The amount of DMSO was detected using a UV detector (Water 2487) at 210 nm and 0.1 mL min<sup>-1</sup> flow rate for 10 min. The amount of residual DMSO in the LevNPs preparation was 0.06%, indicating no toxicity in further experiments.

For analyzing the physicochemical characteristics of LevNPs, the hydrodynamic diameter, PDI, and zeta potential were determined using a Zetasizer (ELSZ-2000, Otsuka, Osaka, Japan). The morphology and structure of LevNPs were observed using TEM (JEM-2100Plus HR, JEOL, Tokyo, Japan). Furthermore, the chemical bonds of the LevNPs were analyzed based on ATR-FTIR (Jasco, Tokyo, Japan) in the spectral range 450–4500 cm<sup>-1</sup>.

To examine the stability of the LevNPs, freeze-dried LevNPs were resuspended in DIW and PBS and monitored at predetermined time points. Changes in the hydrodynamic diameter and PDI were observed after 0, 1, 2, 3, and 4 weeks of storage in PBS at 37 °C under a constant 100 rpm.

**In Vitro Cytotoxicity of LevNPs:** Chondrocytes were cultured in DMEM supplemented with 10% FBS and 1% penicillin-streptomycin. These cells were seeded at a density of 10 000 cells per well in 100  $\mu$ L DMEM in a 96-well plate and cultured overnight in a humidified incubator containing an atmosphere of 5% CO<sub>2</sub> and 95% air at 37 °C. The cells were incubated with LevNPs (0–2 mg mL<sup>-1</sup>) for the indicated time periods. Next, the supernatant was aspirated and replaced with a fresh medium containing 10% CCK-8 (Cell Counting Kit-8; Dojindo Laboratories, Kumamoto, Japan). To analyze the toxicity of LevNPs toward chondrocytes, a lactate dehydrogenase (LDH) colorimetric assay kit (BioVision, Inc., Milpitas, CA, USA) was used according to the manufacturer's instructions. Percentage cytotoxicity was determined using the following formula: (sample LDH – negative control)/(maximum LDH – negative control)  $\times$  100. Absorbance (450 and 595 nm) was measured using a microplate reader (VICTOR X3; PerkinElmer, Waltham, MA, USA).

**Reverse Transcription Polymerase Chain Reaction and Quantitative Reverse Transcription Polymerase Chain Reaction:** Mouse articular chondrocytes were scraped and homogenized. Total RNA isolated from the primary articular chondrocytes using TRIzol (Molecular Research Center, Inc., Cincinnati, OH, USA) was reverse-transcribed into cDNA using random hexamers and reverse transcriptase (Toyobo, Osaka, Japan), and the relative gene expression was assessed using quantitative reverse transcription-PCR (StepOnePlus Real-Time PCR System, Applied Biosystems, Foster City, CA, USA) and SYBR premix Ex Taq (TaKaRa Bio, Shiga, Japan). GAPDH was used for normalization to quantify relative gene expression. The gene-specific primer sets,

annealing temperatures, and cycles are listed in Table S2, Supporting Information.

**Western Blotting:** Total chondrocyte lysate was prepared in lysis buffer (150 mM NaCl, 1% NP-40, 50 mM Tris, 5 mM NaF) supplemented with protease inhibitors and phosphatase inhibitors (Roche, Basel, Switzerland). Anti-COX2 (SC-1745; Santa Cruz Biotechnology, Dallas, TX, USA), CD44 (BD Biosciences, Franklin Lakes, NJ, USA), and ERK1/2 (610408; BD Biosciences) antibodies were used to detect cellular proteins. Total ERK was used as the loading control.<sup>[26]</sup>

**Explant Culture and Alcian Blue Staining:** For cartilage ex vivo culture, cartilage explants were obtained from mouse knee joints, cultured in DMEM (Gibco), and exposed to IL-1 $\beta$  and LevNPs for 36 h simultaneously or LevNPs treated ex vivo-cultured cartilage for 12 h after IL-1 $\beta$  exposure for 24 h. The accumulation of sulfated proteoglycans was assessed using Alcian blue staining (stained with 0.3% Alcian blue 8GX in 3% acetic acid and de-stained with 1N HCl).

**DMM and Intra-Articular Injection:** Experimental OA was induced by DMM surgery in 10–12-week-old male mice. Incising the medial meniscotibial ligament with a surgical blade results in DMM. Following DMM, the medial displacement of the medial meniscus occurred, and weight-bearing on the smaller area resulted in increased local mechanical stress. As the mouse knee is bent during weight-bearing, this generates a greater force on the posterior femur and central tibia, predominantly on the medial side. Sham surgery, in which the ligament was visualized but not transected, was performed on the control joint. PBS and LevNPs (50 mg kg<sup>-1</sup>) were injected via the intra-articular route into the cartilage 4 weeks after DMM surgery. The intra-articular injection was performed once per week for 6 weeks. The mice were euthanized 10 weeks after DMM surgery for histological analysis.

**Cartilage Tissue Histology, Immunohistochemistry Analyses, and Fluorescence Distribution Analyses:** Cartilage samples from the mice were fixed in paraformaldehyde (PFA), decalcified for 2 weeks, trimmed, and embedded in paraffin. Prepared sections (5-micrometer thick) were stained with 0.1% safranin-O and 0.025% fast green. Each section was imaged and scored in accordance with the OARS grading system. The expression patterns of COX2 (SC-1745; Santa Cruz Biotechnology, Dallas, Texas, USA), I $\kappa$ B (#9242, Cell Signaling Technology, Danvers, MA, USA), and CD44 (BD Biosciences, CA, USA) in the cartilage were evaluated using immunohistochemistry. Protein expression was detected using an appropriate AEC+ high sensitivity Substrate Chromogen Ready-to-Use (DAKO, Santa Clara, CA, USA). The sections were viewed using a Nikon Eclipse Ni microscope (Tokyo, Japan). To determine the penetration depth of the LevNPs into the cartilage, the explanted cartilage was exposed to Cy5.5-labeled LevNPs and free Cy5.5. Cultured cartilage was sectioned and observed under an LSM980 NLO microscope (Zeiss, Oberkochen, Germany). To determine the retention time of levan in the knee joint, Cy5.5-labeled LevNPs (10 mg kg<sup>-1</sup>) and free Cy5.5 were intra-articularly injected into the knee joints of C57BL/6 mice ( $n = 3$ ), and their retention times were observed using the eXplore Optix system (Advanced Research Technologies, Montreal, Canada). For double immunofluorescence labeling in cartilage and chondrocyte sections, CD44 (BD Biosciences, CA, USA), NHE3 (Abcam, Cambridge, UK), p-I $\kappa$ B (R&D Systems, Minneapolis, MN, USA), and COX2 (SC-1745; Santa Cruz Biotechnology, Dallas, Texas, USA) primary antibodies were used, followed by incubation with Alexa Fluor 594 anti-rabbit IgG, Alexa Fluor 488 anti-rabbit IgG-conjugated secondary antibody, or Alexa Fluor 488 anti-mouse IgG-conjugated secondary antibody (Thermo Fisher Scientific, Waltham, MA, USA).

**Confocal Microscopy Imaging of the Cartilage:** Cy5.5-labeled LevNPs (10 mg kg<sup>-1</sup>) and free Cy5.5 (equal amount of Cy5.5 as in Cy5.5-labeled LevNPs) were intra-articularly injected into the knee joint using Hamilton syringes, the knee joints of the mice were excised (other tissues were trimmed) and fixed in 4% PFA. Images were obtained from the top of the cartilage using an LSM980 NLO system (Zeiss).

**Protein Microarray:** Protein microarray data were generated using the HuProt Human Proteome Microarray v3.1 (CDI Laboratories). The protein ChIP was equilibrated with the microarray buffer (137 mM NaCl;

2.7 mM KCl; 4.3 mM Na<sub>2</sub>HPO<sub>4</sub>; 1.8 mM KH<sub>2</sub>PO<sub>4</sub>, pH 7.4; 0.05% Triton X-100) for 5 min at room temperature and then incubated in blocking solution (5% filtered skim milk in microarray buffer) for 1 h at 25 °C. To screen for LevNP-binding proteins, the blocked protein ChIP was washed three times with the microarray buffer for 10 min, followed by incubation with free Cy5 or Cy5-labeled LevNPs (5 µg mL<sup>-1</sup>) in PBS for 3 h at 25 °C. Prior to scanning, the protein ChIPs were washed three times with the microarray buffer and drained via centrifugation at 200 × g for 2 min using a 50 mL conical tube. Finally, the protein ChIP was scanned using a GenePix 4000 B instrument (Molecular Devices, Sunnyvale, CA, USA). GST antibody was used to probe all proteins spotted on the ChIPs with Alexa Fluor goat-anti-rabbit 546 conjugated secondary antibody (Invitrogen, Carlsbad, CA, USA). The SNR of each spot was determined as the ratio of the foreground-to-background signals and normalized with the GST signal intensity. The mean signal intensity of all proteins on the ChIP was calculated.

**In Silico Chemical-Protein Binding Assay:** Homology modeling of CD44 (accession ID: NP\_000 601.3) was performed using I-TASSER (<https://zhanglab.ccmb.med.umich.edu/I-TASSER>).<sup>[27]</sup> The 3D chemical structure of levan (PubChem ID: 440 946) was obtained from PubChem (<https://pubchem.ncbi.nlm.nih.gov>). Computational docking simulations between CD44 and levan were conducted using AutoDock Vina (ver.1.1.2).<sup>[28]</sup> The best model score revealed a binding affinity of −5.0 kcal mol<sup>-1</sup>. Protein modeling revealed that levan was bound to the N-terminus of CD44. A graphical representation of the docking structures was generated using PyMOL (ver. 1.3, DeLano Scientific, South San Francisco, CA, USA).

**Statistical Analysis:** All experiments were performed in greater than triplicate ( $n > 3$ ). The resulting data were expressed as the mean ± standard deviation. Differences between groups were compared using the Student's *t*-test, one-way ANOVA with Bonferroni's post-hoc test, Kruskal–Wallis test followed by the Mann–Whitney U test, and two-tailed *t*-test. Statistical analyses were performed using PRISM 7 and  $p \leq 0.05$  was considered significant. *p*-values higher than 0.05 and lower than 0.05, 0.01, and 0.001 are denoted by \*, \*\*, \*\*\*, and \*\*\*\*, respectively, to indicate the level of significance.

## Supporting Information

Supporting Information is available from the Wiley Online Library or from the author.

## Acknowledgements

C.C. and J.S.L. contributed equally to this work. This work was supported by grants from National Research Council of Science & Technology (NST) grant by the Korea government (MSIT) (CRC21021), the National Research Foundation of Korea (SRC-2017R1A5A1014560, NRF-2020R1A2C2004988, NRF-2021M3E5E7023867, NRF-2021M3E5E7023855, NRF-2022R1A2C2004343, and NRF-2022R1A2C4002058), KRIBB (KGM1711134081), and the Korea Healthcare Technology R&D project of the Korea Health Industry Development Institute (HI16C0992).

## Conflict of Interest

The authors declare no conflict of interest.

## Data Availability Statement

The data that support the findings of this study are available in the supplementary material of this article.

## Keywords

CD44, levan, mouse models, nanoparticles, osteoarthritis

Received: April 6, 2022

Revised: June 3, 2022

Published online: June 26, 2022

- [1] A. R. Jordan, R. R. Racine, M. J. Hennig, V. B. Lokeshwar, *Front. Immunol.* **2015**, 6, 182.
- [2] L. J. Kang, Y. Yoon, J. G. Rho, H. S. Han, S. Lee, Y. S. Oh, H. Kim, E. Kim, S. J. Kim, Y. T. Lim, J. H. Park, W. K. Song, S. Yang, W. Kim, *Biomaterials* **2021**, 275, 120967.
- [3] D. J. Hunter, D. Schofield, E. Callander, *Nat. Rev. Rheumatol.* **2014**, 10, 437.
- [4] P. Teriete, S. Banerji, M. Noble, C. D. Blundell, A. J. Wright, A. R. Pickford, E. Lowe, D. J. Mahoney, M. I. Tammi, J. D. Kahmann, I. D. Campbell, A. J. Day, D. G. Jackson, *Mol. Cell* **2004**, 13, 483.
- [5] R. C. Gupta, R. Lall, A. Srivastava, A. Sinha, *Front. Vet. Sci.* **2019**, 6, 192.
- [6] A. Mero, M. Campisi, *Polymers* **2014**, 6, 346.
- [7] Z. Y. Yao, J. Qin, J. S. Gong, Y. H. Ye, J. Y. Qian, H. Li, Z. H. Xu, J.-S. Shi, *Carbohydr. Polym.* **2021**, 264, 118015.
- [8] P. Maudens, S. Meyer, C. A. Seemayer, O. Jordana, E. Allémann, *Nanoscale* **2018**, 10, 1845.
- [9] C. Li, X. You, X. Xu, B. Wu, Y. Liu, T. Tong, J. Chen, Y. Li, C. Dai, Z. Ye, X. Tian, Y. Wei, Z. Hao, L. Jiang, J. Wu, M. Zhao, *Adv. Sci.* **2022**, 9, 2104134.
- [10] X. You, L. Wang, L. Wang, J. Wu, *Adv. Funct. Mater.* **2021**, 31, 2100805.
- [11] K. Ou, X. Xu, S. Guan, R. Zhang, X. Zhang, Y. Kang, J. Wu, *Adv. Funct. Mater.* **2020**, 30, 1907857.
- [12] A. D. Sezer, H. Kazak, E. T. Öner, J. Akbuğa, *Carbohydr. Polym.* **2011**, 84, 358.
- [13] J. C. Park, D. H. Kim, Y. H. Song, H. J. Cha, J. H. Seo, *ACS Appl. Mater. Interfaces* **2020**, 12, 38899.
- [14] M. A. Esawy, E. F. Ahmed, W. A. Helmy, N. M. Mansour, W. M. El-Senousy, M. M. El-Safy, *Carbohydr. Polym.* **2011**, 86, 823.
- [15] R. Srikanth, G. Siddhartha, C. H. S. S. Reddy, H. B. S. M. J. Ramaiah, K. B. Uppuluri, *Carbohydr. Polym.* **2015**, 123, 8.
- [16] J. Zhang, X. Yue, Y. Zeng, E. Hua, M. Wang, Y. Sun, *Biotechnol. Equip.* **2018**, 32, 1583.
- [17] T. Murakami, S. Otsuki, Y. Okamoto, K. Nakagawa, H. Wakama, N. Okuno, M. Neo, *Connect. Tissue Res.* **2019**, 60, 117.
- [18] K. Saravanakumar, A. Sathiyaseelan, A. V. Mariadoss, M.-H. Wang, *Ceram. Int.* **2021**, 47, 8618.
- [19] T. Li, X. Hu, Q. Fan, Z. Chen, Z. Zheng, R. Zhang, *Int. J. Nanomed.* **2020**, 15, 5017.
- [20] S. Georgitsopoulou, A. Angelopoulou, L. Papaioannou, V. Georgakilas, K. Avgoustakis, *J. Drug Delivery Sci. Technol.* **2022**, 67, 102971.
- [21] J. Małaczewska, E. Kaczorek-Lukowska, B. Kaziński, *BMC Vet. Res.* **2021**, 17, 198.
- [22] H. Kuznietsova, I. Byelinska, N. Dziubenko, O. Lynchak, D. Milokhov, O. Khilya, N. Finiuk, O. Klyuchivska, R. Stoika, V. Rybalchenko, *Mol. Cell. Biochem.* **2021**, 476, 3021.
- [23] L. J. Kang, E. S. Kwon, K. M. Lee, C. Cho, J. I. Lee, Y. B. Ryu, T. H. Youm, J. Jeon, M. R. Cho, S. Y. Jeong, S. R. Lee, W. Kim, S. Yang, *Br. J. Pharmacol.* **2018**, 175, 4295.
- [24] L. Kandel, G. Agar, O. Elkayam, A. Sharipov, O. Slevin, G. Rivkin, M. Dahan, V. Aloush, A. B. Pyeser, Y. Brin, Y. Beer, A. Yayon, *Heliyon* **2020**, 6, 04475.

- [25] K. Y. Choi, H. S. Han, E. S. Lee, J. M. Shin, B. D. Almquist, D. S. Lee, J. H. Park, *Adv. Mater.* **2019**, *31*, 1803549.
- [26] E. V. Tchetina, J. A. Di Battista, D. J. Zukor, J. Antoniou, A. R. Poole, *Arthritis Res. Ther.* **2007**, *9*, R75.
- [27] W. Knudson, A. G. Chow, C. B. Knudson, *Matrix Biol.* **2002**, *1*, 15.
- [28] S. Gou, Y. Huang, Y. Wan, Y. Ma, X. Zhou, X. Tong, J. Huang, Y. Kang, G. Pan, F. Dai, B. Xiao, *Biomaterials* **2019**, *212*, 39.
- [29] H. J. Sim, C. Cho, H. E. Kim, J. Y. Hong, E. K. Song, K. Y. Kwon, D. G. Jang, S. J. Kim, H. S. Lee, C. Lee, T. Kwon, S. Yang, T. J. Park, *Sci. Adv.* **2022**, *8*, abl4222.
- [30] J. Jeon, H. J. Noh, H. Lee, H. H. Park, Y. J. Ha, S. H. Park, H. Lee, S. J. Kim, H. C. Kang, S. I. Eyun, S. Yang, Y. S. Kim, *Ann. Rheum. Dis.* **2020**, *79*, 1635.
- [31] V. Tergaonkar, V. Bottero, M. Okawa, Q. Li, I. M. Verma, *Mol. Cell. Biol.* **2003**, *23*, 8070.